Nowcasting Thunderstorm Anvil Clouds over Kennedy Space Center and Cape Canaveral Air Force Station

David A. Short

ENSCO, Inc., Cocoa Beach, and Applied Meteorology Unit, NASA, Kennedy Space Center, Florida

James E. Sardonia

45th Weather Squadron, U.S. Air Force, Patrick Air Force Base, Florida

Winifred C. Lambert and Mark M. Wheeler

ENSCO, Inc., Cocoa Beach, and Applied Meteorology Unit, NASA, Kennedy Space Center, Florida

ABSTRACT

Electrified thunderstorm anvil clouds extend the threat of natural and triggered lightning to space launch and landing operations far beyond the immediate vicinity of thunderstorm cells. The deep convective updrafts of thunderstorms transport large amounts of water vapor, supercooled water droplets, and ice crystals into the upper troposphere, forming anvil clouds, which are then carried downstream by the prevailing winds in the anvil-formation layer. Electrified anvil clouds have been observed over the space launch and landing facilities of the John F. Kennedy Space Center and Cape Canaveral Air Force Station (CCAFS), emanating from thunderstorm activity more than 200 km away. Space launch commit criteria and flight rules require launch and landing vehicles to avoid penetration of the nontransparent portion of anvil clouds. The life cycles of 163 anvil clouds over the Florida peninsula and its coastal waters were documented using *Geostationary Operational Environmental Satellite* (*GOES*)-*8* visible imagery on 49 anvil-case days during the months of May–July 2001. Anvil clouds were found to propagate at the speed and direction of upper-tropospheric winds in the layer from 300 to 150 hPa, approximately 9.4–14 km in altitude, with an effective average transport lifetime of approximately 2 h and a standard deviation of approximately 30 min. The effective lifetime refers to the time required for the nontransparent leading edge of an anvil cloud to reach its maximum extent before beginning to dissipate. The information about propagation and lifetime was incorporated into the design, construction, and implementation of an objective short-range anvil forecast tool based on upper-air observations, for use on the Meteorological Interactive Data Display System within the Range Weather Operations facility of the 45th Weather Squadron at CCAFS and the Spaceflight Meteorology Group at Johnson Space Center.

1. Introduction

Anvil clouds are formed in the upper troposphere from a supply of water vapor, supercooled cloud droplets, and ice crystals that is carried aloft by the deep convective updrafts of thunderstorms (e.g., Heymsfield 1986). Anvil cirrus is perhaps the most familiar term used for the upper portion of mature and dissipating thunderstorms with *incus,* or anvil, features. However, a variety of terms are in common usage, varying to fit descriptions of the environment and life history of the system being studied. The following paragraphs are intended to distinguish between some of the more common anvil terms and to clarify how they may relate to

the threats of natural and triggered lightning to space launch and landing operations.

The majority of anvil clouds observed in this study showed propagation and lifetime characteristics dominated by low-to-moderate upper-level shear. In some regard, they were similar to the anvil clouds studied by Heymsfield and Blackmer (1988), especially those generated by isolated storms, in that the relationship between the point of origination and subsequent advection/propagation was relatively simple. However, the focus of Heymsfield and Blackmer (1988) was on anvil structure, specifically, the so-called V feature and thermal couplets in satellite infrared observations associated with severe weather and strong vertical wind shear in the Midwest. Thunderstorm activity associated with strong vertical wind shear also occurs in Florida, westerly shear being correlated with severe weather (Hagemeyer and Schmocker 1991).

Corresponding author address: David A. Short, ENSCO, Inc., 1980 N. Atlantic Ave., Suite 230, Cocoa Beach, FL 32931.
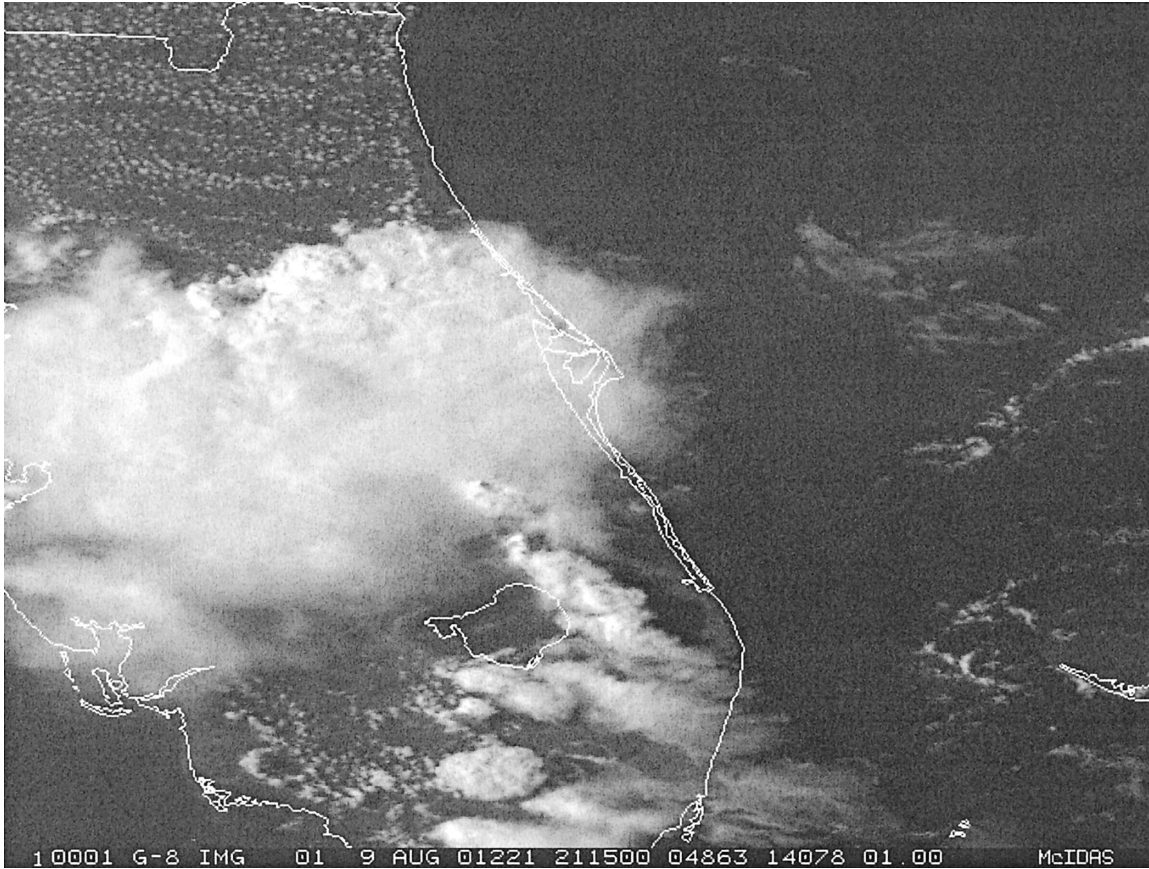E-mail: short.david@ensco.com

FIG. 1. A *GOES-8* visible image at 2115 UTC (1715 EDT) on the afternoon of 9 Aug 2001. Anvil clouds that forced the STS-105 launch to be postponed can be seen over the Cape Canaveral area (center of the image), emanating from a thunderstorm complex to the northwest.

Easterly shear can also result in high-level anvil clouds over the space launch and landing facilities of the John F. Kennedy Space Center (KSC) and Cape Canaveral Air Force Station (CCAFS) on Florida's east coast, originating from convective systems over the Atlantic Ocean. Caniaux et al. (1994) used the term ''forward anvil clouds'' to describe the westward-propagating anvil of a tropical squall line in easterly shear with an easterly jet near 13-km altitude.

Florida also experiences much thunderstorm activity in low-shear environments, resulting in mesoscale convective systems with a distinct convective-to-stratiform life cycle (Yuter and Houze 1995). The stratiform precipitation, recent and/or nearby thunderstorm activity, and thick anvil-cloud layers extending above the freezing level are highly restrictive to space launch and landing activities and are sufficient to scrub an operation.

Tropical mesoscale convective systems and squall lines can also produce an extensive area of clouds and precipitation behind the active convection. The terms precipitating anvil (Zipser 1977), trailing stratiform anvil (Smull 1995), and *nimbostratus cumulonimbogenitous* (Brown 1979) have been used to describe these precipitating cloud systems.

Braun and Houze (1996) used the term ''overhanging'' anvil to describe nonprecipitating anvil clouds generated by a Midwest squall line. Low-shear environments can produce electrified, overhanging upper-level anvil clouds, although their horizontal propagation appears to be limited to a few tens of kilometers from the thunderstorm cells that generated them. Figure 1 shows an example of anvil clouds over the KSC/CCAFS area in a low-shear environment, originating from a complex of thunderstorms to the northwest. The Spaceflight Meteorology Group (SMG) postmission summary for the Space Transportation System mission 105 (STS-105, the

TABLE 1. Climatological pressures and heights of tropopause and 300- and 150-hPa surfaces at KXMR for the months of May, Jun, and Jul. The values were developed from a 20-y database (1973–92) by the Range Commanders Council Meteorology Group (online at http://www.edwards.af.mil/weather/rcc.htm).

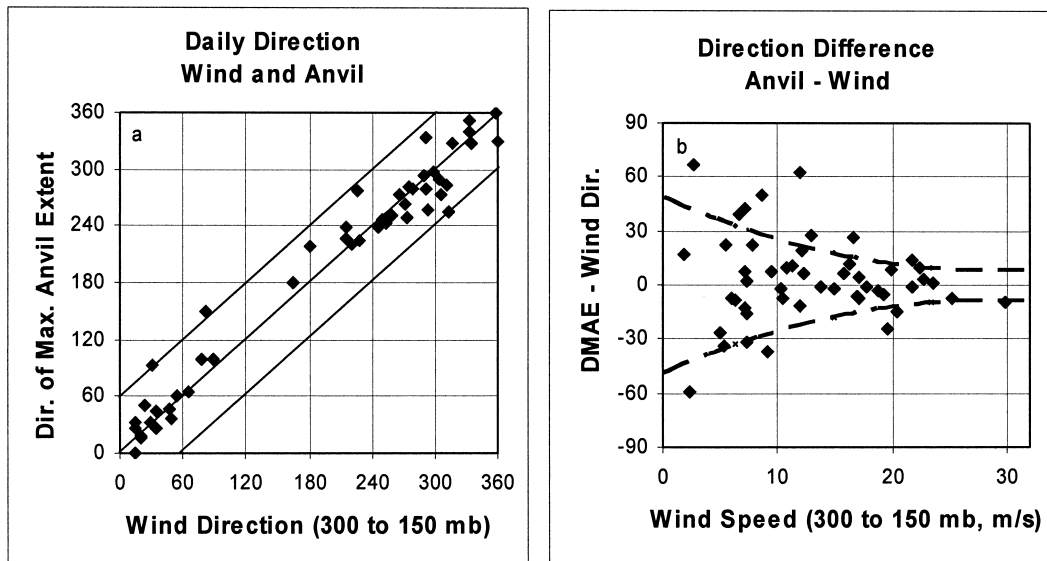| Month	Tropopause pressure (hPa)	Tropopause height (km)	150-hPa height (km)	300-hPa height (km)	150–300-hPa thickness (km)
May	142	14.5	14.0	9.6	4.4
Jun	129	15.1	14.1	9.7	4.4
Jul	128	15.1	14.2	9.7	4.5

FIG. 2. (a) Daily DMAE vs upper-level wind direction and (b) deviation of DMAE from wind direction vs upper-level wind speed. Note that the deviations are largest at the lowest wind speeds. The dashed lines in (b) indicate trends of ±1 std dev, estimated from difference statistics for the three intervals of 0–10, 10–20, and 20–30 m s^{-1}.

space shuttle), reported that although no rain was reported at KSC, thunderstorms were close enough to the return-to-launch-site emergency-landing approaches to halt the launch countdown. In addition, the anvil cloud from the thunderstorms had moved overhead of both the shuttle landing facility and the launch pad, violating both the flight rules (FR) for emergency landings and the launch commit criteria (LCC).

Electrified anvil clouds have been observed over the KSC/CCAFS area emanating from thunderstorm activity over the Gulf of Mexico, more than 200 km away, in environments with strong westerly shear. Mature anvils and even detached anvils can remain electrically charged for several hours, posing the threat of triggered lightning if penetrated by a launch or landing vehicle (Garner et al. 1997).

An airborne field-mill project (hereinafter KSC ABFM 2000) has been designed and conducted to sample electrical fields within thunderstorm anvil clouds in the KSC/CCAFS area and to determine the time scale for decay of the field (Merceret and Christian 2000). The objectives of KSC ABFM 2000 were to provide new information to the Lightning Advisory Panel (Krider et al. 1999) that reviews and formulates natural and triggered lightning LCC for space launch and landing activities.

Charging mechanisms in anvil clouds are complex. However, the general structure is a positively charged center surrounded by negatively charged exterior-screening layers near the top and bottom of the anvil cloud (Marshall et al. 1989). The screening layers can have an adverse effect on the ability of the ground-based Launch Pad Lightning Warning System (Harms et al. 1997) to detect electrification in an anvil cloud above

the network. Real-time operational decisions are based on an imperative to avoid launch and landing through the optically nontransparent portions of anvil clouds. A comprehensive set of LCC (Roeder et al. 1999) for space launches of unmanned rockets and the space shuttle are used by the 45th Weather Squadron launch weather officers (LWO) and FRs are used for the space shuttle by the SMG. The LCC and FRs assure that space-flight vehicles remain well clear of such potentially hazardous clouds. The LWOs have identified anvil forecasting as one of their most challenging tasks when attempting to predict the probability of a triggered lightning LCC violation. The goal of this study was to develop an objective nowcasting technique to determine if the KSC/CCAFS area would be affected by nontransparent anvil clouds.

2. Data and analysis procedures

The primary sources of data for this study were images of visible and infrared radiation from the *Geostationary Operational Environmental Satellite* (*GOES*)-*8* and vertical profiles of wind speed, wind direction, temperature, and dewpoint from the operational radiosonde network. Lightning data from the Cloud-to-Ground Lightning Surveillance System (Harms et al. 1997), a local sferics-based system, were also used to verify the locations of active thunderstorm cells.

Anvil-cloud properties were measured subjectively in an analysis of visible imagery from channel 1 on *GOES-8* (0.55–0.75 μm) with a spatial resolution of 1 km. *GOES-8* data were archived every 15–30 min and were analyzed using the Man Computer Interactive Data Ac-
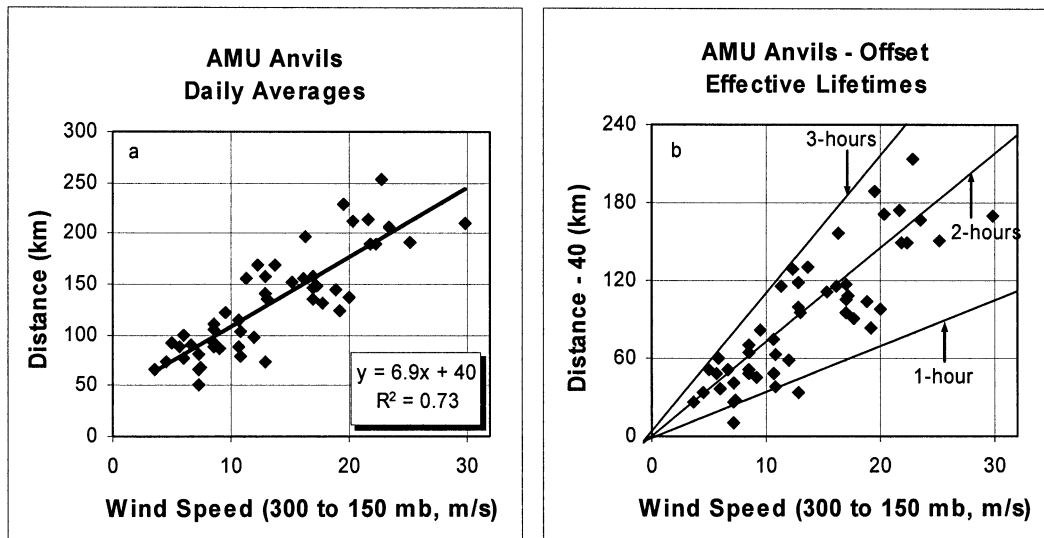
FIG. 3. (a) Daily averages of wind speed vs anvil distance and (b) daily averages of wind speed vs anvil distance minus offset. The 40-km offset used in (b) was determined from the linear regression in (a). The sloping lines in (b) denote effective transport lifetimes, calculated from the ratio of distance offset to wind speed.

cess System (McIDAS;[1] Smith 1975). The McIDAS software provides the user with customized image enhancement capabilities that facilitate interpretation of cloud features in the satellite imagery. Anvil clouds originating from small clusters of thunderstorms were readily evident in time loops of visible imagery.

These anvil clouds, consistent with the classification *cirrostratus cumulonimbogenitus,* rapidly expanded tens of kilometers or more in accord with the wind flow in the upper troposphere, in the layer from about 300 to 150 hPa. Down-shear anvil clouds are highly reflective to visible radiation during their growing and mature phases, being composed of ice, primarily in the form of vapor-grown ice crystals and crystal aggregates (Black and Hallett 1998). Such optically nontransparent anvil clouds obscure views of the surface and lower clouds. Infrared imagery (channel 4, 10.2–11.2 μm) indicated radiative temperatures of less than 240 K at the tops of anvil clouds, consistent with atmospheric temperatures in the upper troposphere.

An anvil-case day was defined as one in which the generation and dissipation of at least three separate anvil clouds were clearly evident and measured from satellite imagery. The objective was to obtain statistics applicable to anvils generated by isolated thunderstorm complexes. From an operational point of view, the maximum forecast benefit can be obtained when such anvils are first generated upstream of the KSC/CCAFS area. For

that reason, anvil clouds that subsequently passed over another thunderstorm complex were not included in this study.

The life history of an anvil cloud was considered to have begun when it first became visible above a thunderstorm complex and was considered complete when its leading nontransparent edge reached a maximum horizontal distance from the point of origin. The direction of maximum anvil extent (DMAE) was measured from the point of origin to the farthest extent of the nontransparent edge. Determination of the location of the nontransparent edge was subjective, with an uncertainty estimated to be about 20 km. The uncertainty was a small fraction of the natural variability associated with observed anvils clouds and is not a significant factor in the analysis. At times, anvil-type clouds that were less than 30-km long were seen in two or three consecutive frames of the *GOES-8* visible imagery before dissipating. Fleeting features of this type were associated with isolated thunderstorm cells, consistent with the classification *cirrus spissatus cumulonimbogenitous,* and did not pose the long-range, long-term space launch and landing threat associated with the anvil clouds included in the analysis presented here.

For each anvil cloud documented in the satellite imagery, the upper-tropospheric wind speed, wind direction, temperature, and dewpoint from 150 to 300 hPa were determined from the nearest radiosonde observation (raob) that preceded anvil formation. Raob data from Florida National Weather Service stations were obtained in near–real time through the National Oceanic and Atmospheric Administration's (NOAA's) NOAA-PORT Broadcast Service (FCM 2001, see chapter 4), and raob data from the CCAFS balloon facility (Inter-

**Average Dewpoint Depression (300-to-150 mb layer)
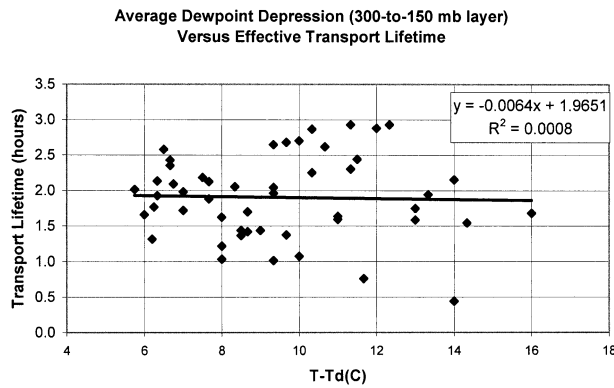Versus Effective Transport Lifetime**

FIG. 4. Daily averages of dewpoint depression vs transport lifetime for the 49 anvil-case days observed during May–Jul 2001. Transport lifetimes were derived from the analysis shown in Fig. 3b. The solid line was determined by linear regression.
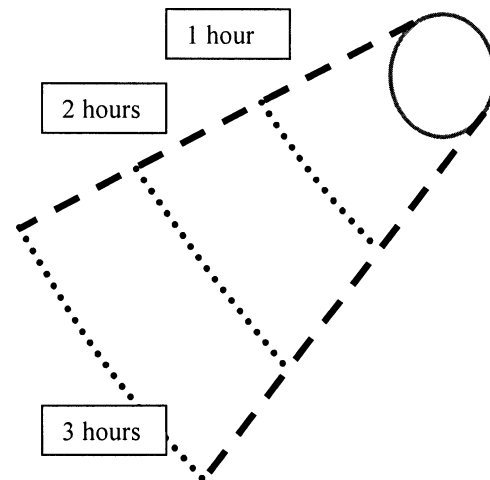

FIG. 5. Schematic representation of an anvil threat sector. The sector is 30° in width, extending toward the southwest from a 40-km circle centered on the station of interest. Arcs are located upstream at distances consistent with 1-, 2- and 3-h transport times by the upper-level winds.

national Civil Aviation Organization identifier KXMR) were obtained through a local data system at CCAFS. Table 1 lists climatological statistics of the 150- and 300-hPa pressure surfaces and the tropopause at KXMR for the months of May, June, and July. The 150-hPa level is the first mandatory level below the average height of the tropopause for the analysis period. The average depth of the 150–300-hPa layer is 4.4 km. The layer includes the climatological height of the equilibrium level (180 hPa) at which convective updrafts reach neutral buoyancy, depositing ice crystals, condensation nuclei, and water vapor, which form the anvil. The average dewpoint depression in the upper-tropospheric layer was also determined.

3. Results

The life cycles of 163 anvils were observed over the Florida peninsula and its costal waters during the months of May, June, and July of 2001 on 49 case days. The DMAEs and lifetimes were sufficiently similar on a given case day that their average values were representative of individual anvils.

Figure 2a shows a scatter diagram of the daily layer-averaged upper-tropospheric wind direction and DMAE for the 49 case days. The diagonal lines indicate the 1:1 line and an envelope of ±60°, which contains most of the data points. The correlation coefficient between the two variables is 0.98, explaining 96% of the variance. This result is encouraging, given the potential 12-h time displacement between raobs and anvil formation/propagation and the potential spatial displacement of up to several hundred kilometers. The layer-averaged upper-level winds were from the southwest through the northeast for most of the case days. The average 300–150-hPa wind direction for the 49 case days was 318°, as compared with 322° for the average DMAE. This value indicates that the upper-level wind direction gives a nearly unbiased indication of the DMAE. The vast majority of points lie close to the 1:1 diagonal, with

two outliers showing discrepancies of more than 60° between the DMAE and the upper-level wind direction.

Figure 2b shows the direction difference between the DMAE and wind direction as a function of upper-tropospheric wind speed. Differences are greatest for lower wind speeds. The standard deviation of differences is 24° overall but is only 11° for wind speeds of greater than 15 m s^{-1}. The dashed lines indicate trends of ±1 standard deviation, estimated by a second-order polynomial fit to difference statistics for the three intervals of 0–10, 10–20, and 20–30 m s^{-1}. This result indicates that the DMAE is more highly correlated with wind direction as the wind speed increases and provides guidance for the width of the threat sector described in detail below.

Figure 3a shows a scatter diagram of daily averages of layer-averaged wind speed in the upper-troposphere versus anvil distance for the 49 anvil-case days. A linear regression between the two variables gives an intercept of 40 km and a slope of 6.9 km m^{-1} s, indicating a time scale of 6900 s = 1.92 h. With a correlation coefficient of 0.85, the regression relation explains 73% of the variance of anvil distance by the wind speed. This statistic confirms the results of an earlier pilot study that had established a high correlation between upper-tropospheric wind speed and anvil transport lifetime (Lambert 2000). The nonzero intercept indicates that anvil clouds can be expected to reach a scale of about 40 km, when the upper-level wind speed is near zero, because of the inertia and divergence of the convective updrafts and their load of hydrometeors.

Figure 3b shows a scatter diagram of wind speed versus anvil length minus the 40-km offset mentioned previously. The solid sloping lines indicate time scales that are consistent with the wind speeds and anvil dis-
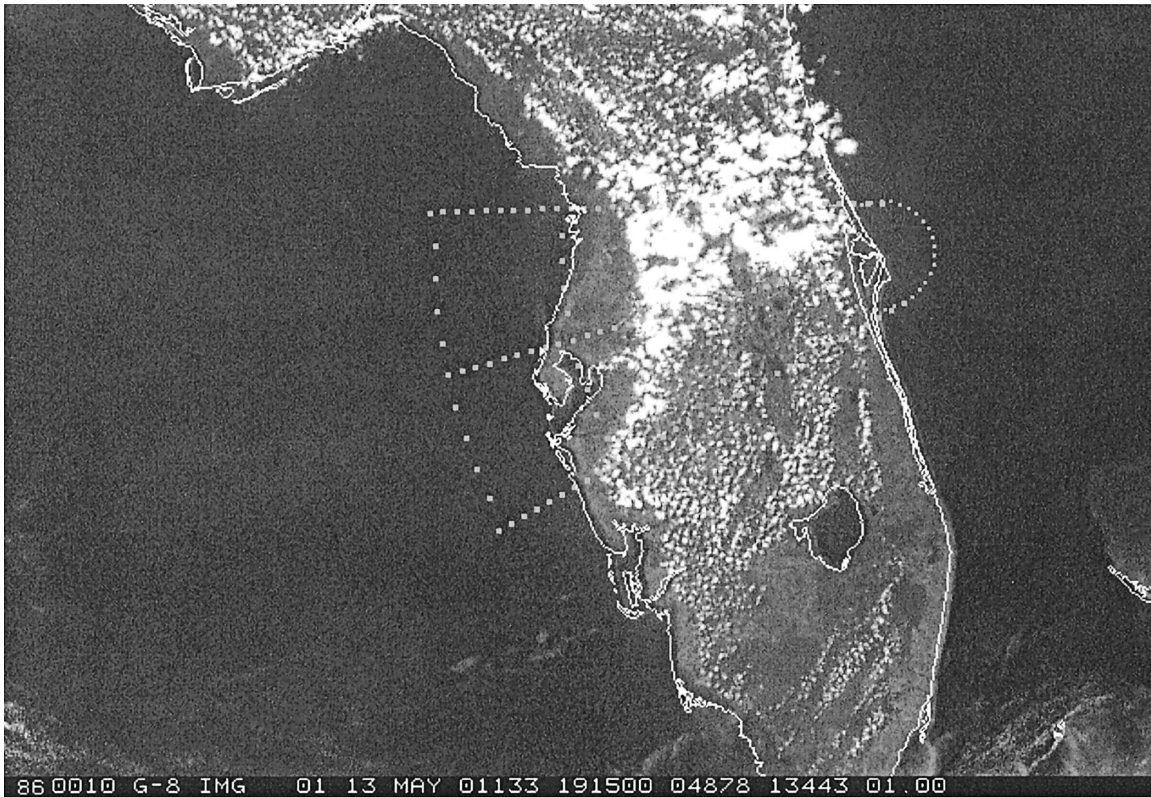
FIG. 6. An example of the anvil forecast graphic overlaid on a visible satellite image of the Florida peninsula. The anvil threat corridor was computed from radiosonde data observed at XMR at 1500 UTC (1100 EDT) 13 May 2001, prior to the onset of convective activity. The satellite image was observed at 1915 UTC (1732 LT) just after the onset of convection in central Florida.

tances. For example, a length offset of 144 km and a speed of 20 m s^{-1} indicate a time scale of 2 h. The time scale is referred to as an effective transport lifetime, indicating the approximate time it took the anvil cloud to reach its maximum extent at maturity. The average effective transport lifetime is 1.92 h, with a standard deviation of 0.58 h.

a. Lower-tropospheric wind speed and direction

Visual inspection of satellite imagery indicated a clear influence of the lower-tropospheric winds on the motion of convective cells and thunderstorms during their developing stages. The average direction of the lower-level winds (900–500 hPa) was 191° as compared with 318° for the average upper-level wind direction for the 49 anvil-case days, with a clockwise rotation with increasing height. The average lower-level wind speed was 5.1 m s^{-1}, as compared with the average upper-level wind speed of 13.5 m s^{-1}.

Figure 2b shows that the difference between DMAE and upper-level wind direction increases as the upper-level wind speed decreases. In an effort to determine whether some of these differences could be accounted for by the lower-level wind field, a weighted vector average direction (WVAD) was computed from the up-

per-and lower-level winds for the 19 case days for which the upper-level wind speed was less than 10 m s^{-1}. As the weight for the lower-level wind was increased from 0.0 to 0.4 while the weight for the upper-level remained at 1.0, the correlation between WVAD and DMAE increased from 0.949 to 0.958, an effect of less than 1%. It was concluded that the lower-tropospheric wind information does provide important clues to the motion of developing convective cells; however, it does not provide sufficient additional information on the subsequent propagation of thunderstorm anvil clouds to justify incorporation into this operational technique for nowcasting the DMAE.

b. Upper-tropospheric humidity

Figure 4 shows a scatter diagram of dewpoint depression versus transport lifetime for the 49 anvil-case days documented in this study. A linear regression gives a correlation coefficient of 0.03 and a slope near zero, both of which indicate no useful relationship between the variables. Nevertheless, it does seem physically plausible that humidity would have an impact on anvil lifetime. This question may be more effectively addressed with an analysis of upper-level humidity fields that have better spatial and temporal continuity and a
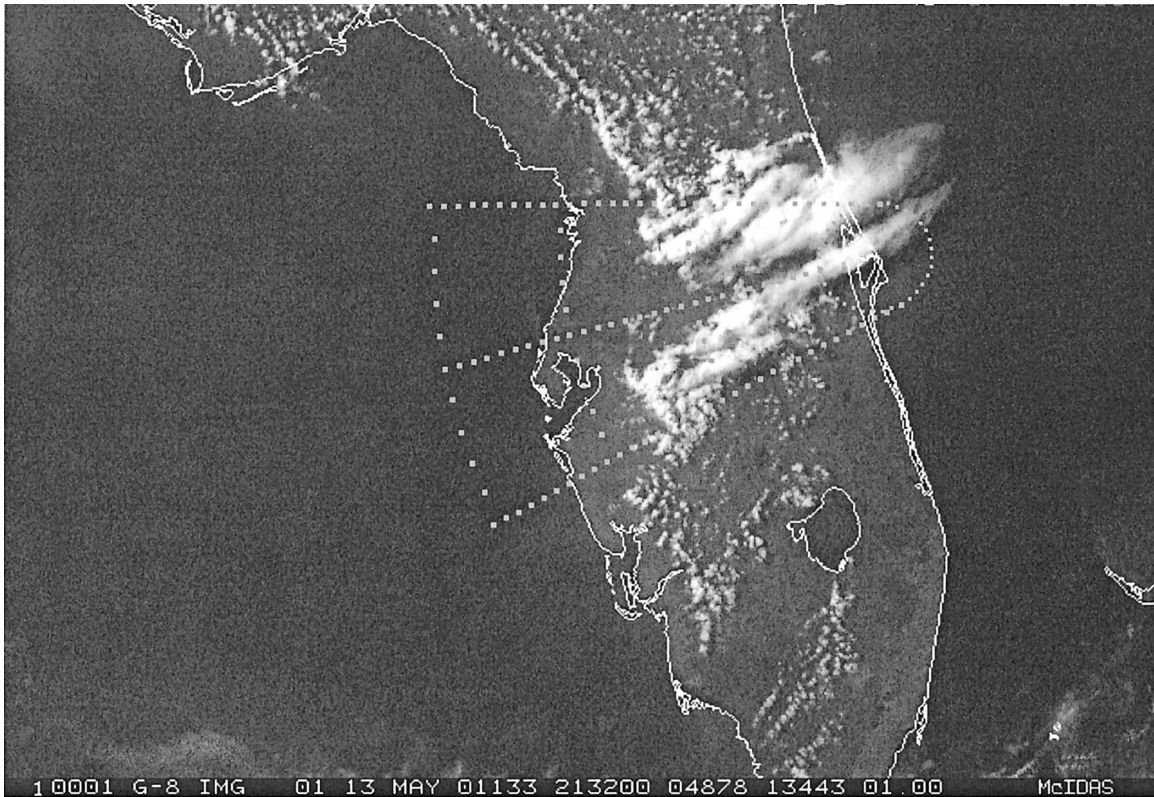
Fig. 7. As in Fig. 6, but for 2132 UTC (1732 EDT). Thunderstorms that formed within the graphical threat sector produced anvil clouds that moved over the KSC/CCAFS area.

humidity sensor with better sensitivity than that provided by the current radiosonde network.

4. Extrapolation/advection forecast tool

The anvil-forecasting tool described below has been implemented on the McIDAS-based Meteorological Interactive Data Display System (MIDDS) to draw automatically an anvil threat sector on top of an image (satellite or radar composite). In the preconvective environment, the threat sector will alert the forecaster to the specific area where anvils from developing thunderstorms could threaten the launch area within a time frame of several hours.

The observational studies documented above indicate that the motion of anvil clouds is highly correlated with the speed and direction of upper-level winds. As a result, a short-term anvil-forecasting tool can be formulated to extrapolate future positions of anvil clouds as they are advected by the upper-level wind field. By combining data into easily understood information, graphical products help to reduce information overload for the meteorologist. If the forecaster expects thunderstorm formation within the threat sector, the anvil clouds from those thunderstorms will likely affect the KSC/CCAFS area and cause violations of the LCC/FR.

Figure 5 shows a schematic representation of an anvil

threat sector. The 40-km standoff circle is consistent with the regression intercept in Fig. 3a and with FRs for the space shuttle, which state that its flight path must be more than 37 km (20 n mi) from opaque anvil clouds (Bauman and Businger 1996). The following threat-sector properties were based on the propagation and lifetime characteristics of thunderstorm anvil clouds observed over Florida and its coastal waters (as discussed above and as shown in Figs. 2a,b and 3a,b) and on experimental testing of the graphical nowcasting tool:

- 40-km standoff circle,
- 30° sector width,
- orientation given by 300–150-hPa average wind direction,
- 1-, 2- and 3-h arcs in upwind direction, and
- arc distances given by 300–150-hPa vector-averaged wind speed.

The Applied Meteorology Unit has developed a short-term anvil-forecasting tool for implementation on MIDDS. The tool, activated by a one-line McIDAS command, is written in Beginner's All-Purpose Symbolic Instruction Code (BASIC) for McIDAS (McBASI) and runs a McBASI script. A ''help'' command for the tool is also available.

Figure 6 shows an example of the anvil-threat-sector graphic overlaid on a visible satellite image of the Flor-

ida peninsula. The anvil threat sector was computed from radiosonde data observed at KXMR at 1500 UTC [1100 eastern daylight time (EDT)] 13 May 2001, prior to the onset of convective activity. The satellite image was observed at 1915 UTC (1732 LT) just after the onset of convection in central Florida.

Figure 7 shows the anvil threat sector as in Fig. 6, but for 2132 UTC (1732 EDT). Thunderstorms that formed within the graphical threat sector produced anvil clouds that moved over the KSC/CCAFS area.

5. Summary and conclusions

The method described herein for the short-term prediction of anvil clouds that are generated by thunderstorm activity and advected from tens to hundreds of kilometers downstream by upper-tropospheric winds was implemented in April of 2002 within the Range Weather Operations facility on CCAFS and the SMG at Johnson Space Center to assist forecasters in nowcasting the threats of natural and triggered lightning to space launch and landing activities at the KSC/CCAFS spaceport. The tool was successfully used to nowcast triggered lightning threats to the launch of STS-111 on 30 May 2002, which was postponed because of encroachment of anvil clouds over the launch complex.

Parameters for the graphical nowcast tool were derived from a study of 163 anvil clouds observed over the Florida peninsula and its coastal waters on 49 case days during May–July 2001. Anvil clouds were found to have an average effective transport lifetime of 2 h with a standard deviation of approximately 30 min. The distance and direction of propagation were consistent with the average wind speed and wind direction in the layer between 300 and 150 hPa, about 9.7–14.1-km altitude, just below the tropopause.

The tool has recently been upgraded to include a capability for using forecast upper-level winds from the Eta and Rapid Update Cycle Models. Possible future work may include an automatic adjustment of the anvil-averaging level for wind speed and direction based on variable thermodynamic considerations such as the equilibrium level and/or the tropopause height.

REFERENCES

Bauman, W. H., III, and S. Businger, 1996: Nowcasting for space shuttle landings at Kennedy Space Center, Florida. *Bull. Amer. Meteor. Soc.,* **77,** 2295–2305.

Black, R. A., and J. Hallett, 1998: The mystery of cloud electrification. *Amer. Sci.,* **86,** 526–534.

Braun, S. A., and R. A. Houze Jr., 1996: The heat budget of a mid-latitude squall line and implications for potential vorticity production. *J. Atmos. Sci.,* **53,** 1217–1240.

Brown, J. M., 1979: Mesoscale unsaturated downdrafts driven by rainfall evaporation: A numerical study. *J. Atmos. Sci.,* **36,** 313–338.

Caniaux, G., J.-L. Redelsperger, and J.-P. Lafore, 1994: A numerical study of the stratiform region of a fast-moving squall line. Part I: General description and water and heat budgets. *J. Atmos. Sci.,* **51,** 2046–2074.

FCM, 2001: National Severe Local Storms operations plan. Office of the Federal Coordinator for Meteorology, Rep. FCM-P11-2001, 98 pp.

Garner, T., R. Lafosse, D. G. Bellue, and E. Priselac, 1997: Problems associated with identifying, observing, and forecasting detached thunderstorm anvils for space shuttle operations. Preprints, *Seventh Conf. on Aviation, Range, and Aerospace Meteorology,* Long Beach, CA, Amer. Meteor. Soc., 302–306.

Hagemeyer, B. C., and G. K. Schmocker, 1991: Characteristics of east-central Florida tornado environments. *Wea. Forecasting,* **6,** 499–514.

Harms, D. E., B. F. Boyd, R. M. Lucci, M. S. Hinson, and M. W. Maier, 1997: Systems used to evaluate the natural and triggered lightning threat to the Eastern Range and Kennedy Space Center. Preprints, *28th Int. Conf. on Radar Meteorology,* Austin, TX, Amer. Meteor. Soc., 240–241.

Heymsfield, A. J., 1986: Ice particle evolution in the anvil of a severe thunderstorm during CCOPE. *J. Atmos. Sci.,* **43,** 2463–2478.

Heymsfield, G. M., and R. H. Blackmer Jr., 1988: Satellite-observed characteristics of Midwest severe thunderstorm anvils. *Mon. Wea. Rev.,* **116,** 2200–2224.

Krider, E. P., H. C. Koons, R. L. Walterscheid, W. D. Rust, and J. C. Willett, 1999: Natural and triggered lightning launch commit criteria (LCC). The Aerospace Corporation Aerospace Rep. TR-99(1413)-1, 15 pp. [Available from the Space and Missile Systems Center, 2430 E. El Segundo Blvd., Los Angeles AFB, CA 90245 as SMC Rep. SMC-TR-99-20.]

Lambert, W. C., 2000: Improved anvil forecasting: Phase I final report. NASA Kennedy Space Center Contractor Rep. CR-2000-208573, 24 pp. [Available from ENSCO, Inc., 1980 N. Atlantic Ave., Suite 230, Cocoa Beach, FL 32931.]

Marshall, T. C., W. D. Rust, W. P. Winn, and K. E. Gilbert, 1989: Electrical structure in two thunderstorm anvil clouds. *J. Geophys. Res.,* **94,** 2171–2181.

Merceret, F. J., and H. Christian, 2000: KSC ABFM 2000—A field program to facilitate safe relaxation of the lightning launch commit criteria for the American space program. Preprints, *Ninth Conf. on Aviation and Range Meteorology,* Orlando, FL, Amer. Meteor. Soc., 447–449.

Roeder, W. P., J. E. Sardonia, S. C. Jacobs, M. S. Hinson, D. E. Harms, and J. T. Madura, 1999: Avoiding triggered lightning threat to space launch from the Eastern Range/Kennedy Space Center. Preprints, *Eighth Conf. on Aviation, Range, and Aerospace Meteorology,* Dallas, TX, Amer. Meteor. Soc., 120–124.

Smith, E. A., 1975: The McIDAS system. *IEEE Trans. Geosci. Electron.,* **GE-13,** 123–136.

Smull, B. F., 1995: Convectively induced mesoscale phenomena in the tropical and warm-season midlatitude atmosphere. *Rev. Geophys.,* **33** (Suppl.), 897–906.

Yuter, S. E., and R. A. Houze Jr., 1995: Three-dimensional kinematic and microphysical evolution of Florida cumulonimbus. Part I: Spatial distribution of updrafts, downdrafts, and precipitation. *Mon. Wea. Rev.,* **123,** 1921–1940.

Zipser, E. J., 1977: Mesoscale and convective-scale downdrafts as distinct components of squall line structure. *Mon. Wea. Rev.,* **105,** 1568–1589.